Solid-state NMR analysis of ligand-receptor interactions reveals an induced misfit in the binding site of isorhodopsin

Creemers, A.F.L.; Bovee-Geurts, P.H.M.; Grip, W.J. de; Lugtenburg, J.; Groot, H.J.M. de

Solid-State NMR Analysis of Ligand−Receptor Interactions Reveals an Induced Misfit in the Binding Site of Isorhodopsin

Alain F. L. Creemers,[‡] Petra H. M. Bovee-Geurts,[§] Willem J. DeGrip,[‡,§] Johan Lugtenburg,[‡] and Huub J. M. de Groot*[,‡]

Leiden Institute of Chemistry, Leiden University, P.O. Box 9502, 2300 RA Leiden, The Netherlands, and Department of Biochemistry, Institute of Cellular Signalling, University of Nijmegen, P.O. Box 9101, 6500 HB Nijmegen, The Netherlands

Received July 9, 2004; Revised Manuscript Received October 5, 2004

ABSTRACT: Rhodopsin is the photosensitive protein of the rod photoreceptor in the vertebrate retina and is a paradigm for the superfamily of G-protein-coupled receptors (GPCRs). Natural rhodopsin contains an 11-*cis*-retinylidene chromophore. We have prepared the 9-*cis* analogue isorhodopsin in a natural membrane environment using uniformly ^{13}C-enriched 9-*cis* retinal. Subsequently, we have determined the complete ^{1}H and ^{13}C assignments with ultra-high field solid-state magic angle spinning NMR. The 9-*cis* substrate conforms to the opsin binding pocket in isorhodopsin in a manner very similar to that of the 11-*cis* form in rhodopsin, but the NMR data reveal an improper fit of the 9-*cis* chromophore in this binding site. We introduce the term "induced misfit" to describe this event. Downfield proton NMR ligation shifts ($\Delta\sigma_{lig}^{H} > 1$ ppm) are observed for the 16,17,19-H and nearby protons of the ionone ring and for the 9-methyl protons. They provide converging evidence for global, nonspecific steric interactions between the chromophore and protein, and contrast with the specific interactions over the entire ionone ring and its substituents detected for rhodopsin. The $\Delta\sigma_{lig}^{C}$ pattern of the polyene chain confirms the positive charge delocalization in the polyene associated with the protonation of the Schiff base nitrogen. In line with the misalignment of the ionone ring, an additional and anomalous perturbation of the ^{13}C response is detected in the region of the 9-*cis* bond. This provides evidence for strain in the isomerization region of the polyene and supports the hypothesis that perturbation of the conjugation around the *cis* bond induced by the protein environment assists the selective photoisomerization.

The rhodopsin visual pigment initiates visual transduction in the mammalian rod photoreceptor cell. In addition, rhodopsin serves as a paradigm for the large and diverse family of seven transmembrane helix G-protein-coupled receptors (GPCRs)[1] that mediate the transduction of signals from the extracellular environment across the membrane to the interior of the cell (*1*). In rhodopsin, 11-*cis*-retinal is covalently bound to the protein via a protonated Schiff base (pSB) linkage to the ϵ-amino group of Lys296 to form the 11-*cis*-retinylidene chromophore with a λ_{max} of 498 nm (*2*−*4*). Absorption of a photon by the chromophore leads to an ultrafast (<200 fs) isomerization of the C11═C12 bond from the 11-*cis* to the all-*trans* configuration (Figure 1) (*5*, *6*). The photoisomerization in rhodopsin proceeds with a quantum yield Φ of 0.67. This means that two of every three photons absorbed are effective in activating the ligand and triggering the visual signal transduction cascade that leads to a nerve pulse in the central nervous system (*7*−*9*).

Although *in vivo* only the 11-*cis* configuration of retinal has been detected in visual pigments, other retinal stereoisomers are also able to generate stable photosensitive pigments upon incubation with the opsin apoprotein (*10*). In particular, administration of 9-*cis*-retinal can be an effective prophylaxis in transgenic mice suffering from photoreceptor degeneration due to a defect in 11-*cis*-retinal synthesis (*11*, *12*). The 9-*cis* isomer can form a pSB with Lys296 in opsin, to form a pigment with a λ_{max} of 485 nm, and act as an inverse agonist that suppresses the activity of the GPCR. The 9-*cis* isorhodopsin analogue photoisomerizes with a Φ of 0.22 into the agonist form, which is the same batho-rhodopsin all-*E* intermediate as for the rhodopsin species (*6*, *13*−*15*). This implies very similar shapes of the binding pockets accommodating the two different chromophore configurations. In contrast, the different λ_{max} values, binding energies, and activation efficiencies suggest a different pattern of protein−ligand interactions for isorhodopsin versus rhodopsin.

* To whom correspondence should be addressed. E-mail: h.groot@chem.leidenuniv.nl. Fax: +31-71-5274603. Telephone: +31-71-5274539.

‡ Leiden University.

§ University of Nijmegen.

[1] Abbreviations: GPCR, G-protein-coupled receptor; SB, Schiff base; pSB, protonated Schiff base; λ_{max}, wavelength of maximum visible absorption; ν_{max}, frequency of maximum visible absorption; Φ, quantum yield; MAS NMR, magic angle spinning nuclear magnetic resonance; $CDCl_3$, deuterated chloroform; TMS, tetramethylsilane; RFDR, radio frequency-driven dipolar recoupling; HetCor, heteronuclear correlation; PMLG, phase-modulated Lee−Goldburg; CP, cross polarization; TPPM, two-pulse phase modulation; σ_{lig}^{H}, isotropic proton shift of the chromophore; σ_{lig}^{C}, isotropic carbon shift of the chromophore; σ_{pSB}^{H}, isotropic proton shift of the pSB model compound; σ_{pSB}^{C}, isotropic carbon shift of the pSB model compound; σ_{lip}^{H}, isotropic proton shift of the phospholipids; σ_{lip}^{C}, isotropic carbon shift of the phospholipids; $\Delta\sigma_{lig}^{H}$, proton NMR ligation shift; $\Delta\sigma_{lig}^{C}$, carbon NMR ligation shift; $\Delta\tilde{\sigma}_{lig}^{H}$, normalized proton NMR ligation shift; $\Delta\tilde{\sigma}_{lig}^{C}$, normalized carbon NMR ligation shift; $\Delta\sigma^{total}$, sum of the $\Delta\sigma_{lig}^{C}$ values of the ^{13}C of the polyene chain.

10.1021/bi048541e CCC: $27.50
Published on Web 11/26/2004

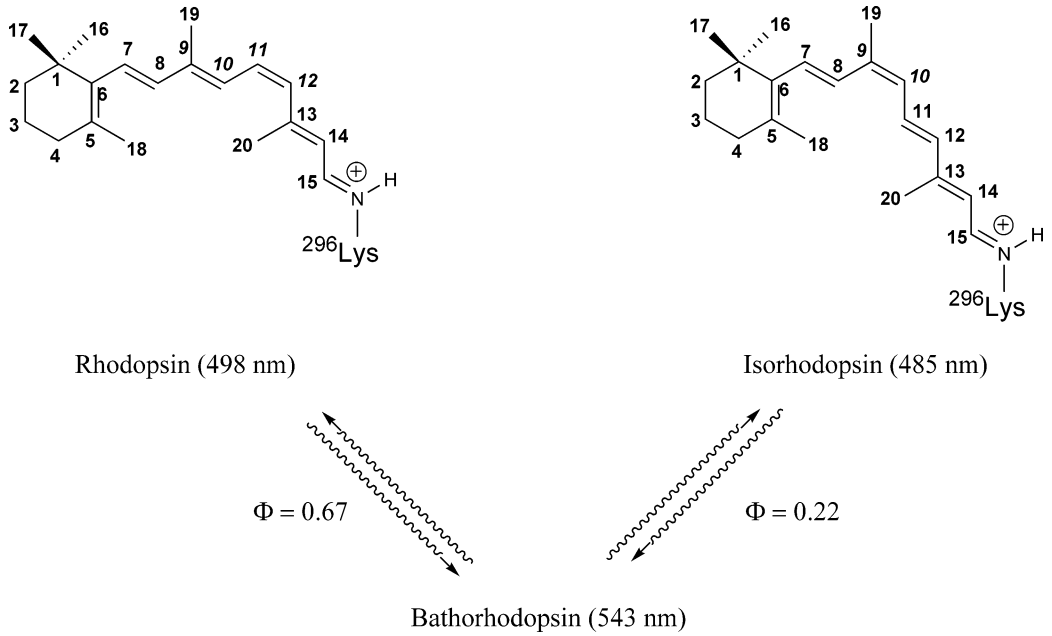

FIGURE 1: Bleaching scheme with the corresponding quantum yield (Φ), formation time, and λ_{max} values of the visual pigments of rhodopsin and isorhodopsin. Even though the pigments have a different ground-state configuration, upon photoexcitation both generate the bathorhodopsin primary photointermediate (*6*).

Recently, a complete proton and carbon assignment of the uniformly ^{13}C-labeled 11-*cis* chromophore bound in the active site of rhodopsin was obtained using two-dimensional (2D) homonuclear (^{13}C−^{13}C) and heteronuclear (^{1}H−^{13}C) MAS NMR correlation spectroscopy (*16*). The data revealed significant and highly localized nonbonding interactions between specific methyl groups of the ring moiety and the surrounding protein residues. In addition, $\Delta\sigma_{lig}^{H}$ and $\Delta\sigma_{lig}^{C}$ for the polyene chain provided evidence for a nonplanar conformation around the 12-s bond due to steric hindrance involving methyl group C20. The NMR shift data reveal accumulation of positive charge in this region (*17*). In line with these results, double-quantum ^{13}C NMR provides convincing evidence for perturbations of the polyene double and single bonds in the vicinity of the isomerization site due to interactions of the ligand with polar residues, leading to the postulation that some strain in the polyene assists the rapid selective photoisomerization of the 11-*cis* bond (*18*).

To study the protein−ligand interactions on the chromophore in isorhodopsin, uniformly ^{13}C-labeled 9-*cis*-retinal is reconstituted into native bovine opsin. A complete ^{1}H and ^{13}C NMR assignment is obtained, and details of the electronic and spatial structure are resolved. In particular, $\Delta\tilde{\sigma}_{lig}^{H}$ and $\Delta\tilde{\sigma}_{lig}^{C}$ reveal significant global protein−ligand interactions that are distinctly different from the specific interactions found previously for rhodopsin. In this way, the NMR data provide converging evidence for an "induced misfit" of the 9-*cis*-retinylidene chromophore of isorhodopsin, which contrasts with the precise fit observed for the chromophore of rhodopsin (*16*). Finally, the isorhodopsin data support the hypothesis that strain in the polyene around the *cis* bond assists the photoisomerization (*18*).

MATERIALS AND METHODS

Uniformly ^{13}C-labeled all-*trans*-retinal was prepared via total organic synthesis from commercially available 99% enriched starting materials (*19*). The material was dissolved in dry acetonitrile and irradiated for 20 h at room temperature with an incandescent lamp, yielding a photostationary mixture of *cis* isomers. 9-*cis*-Retinal was separated from the mixture with HPLC (*20*). The integrity and purity of the uniformly ^{13}C-labeled 9-*cis*-retinal were verified with 600 MHz ^{1}H NMR ($CDCl_3$) and 150 MHz ^{1}H noise-decoupled ^{13}C NMR ($CDCl_3$) (*21*). To prepare isorhodopsin samples, rod outer segment membranes containing opsin were isolated from approximately 40 fresh cattle eyes (*22*). All subsequent manipulations were carried out in the dark or in dim red light filtered to a λ of >620 nm with a long-pass Schott RG620 filter. The opsin was reconstituted with a 2-fold excess of the uniformly ^{13}C-labeled 9-*cis*-retinal. The sample was washed with cyclodextrin to extract the remaining free retinal (*23*). The efficiency of regeneration was determined using the same spectroscopic procedure that is generally applied for rhodopsin (*24*). The calculated A_{280}/A_{485} ratio of 1.9 ± 0.1 corresponds with an efficiency of regeneration of more than 95%. An isorhodopsin sample (15 mg) containing the uniformly ^{13}C-labeled chromophore (0.4 μmol, 0.25 cm^3) was concentrated by centrifugation and loaded into a 4 mm zirconium oxide rotor that was sealed with a Kel-F cap.

NMR spectra were recorded with a Bruker DSX-750 spectrometer (Bruker, Karlsruhe, Germany) equipped with a 4 mm triple-resonance probe, and operating at a ^{1}H frequency of 750 MHz. In earlier NMR studies, it was demonstrated that the application of a radio frequency of 750 MHz significantly contributes to improving the resolution of both one-dimensional (1D) and 2D spectra compared to instruments that operate at lower radio frequencies (*25*, *26*). In addition, due to the high-field frequency, clear nearest neighbor correlation signals are recorded in a relatively short period of time. In approximately 14 h, one RFDR spectrum was recorded; a similar experiment at a radio frequency of 400 MHz takes approximately 48 h.

All NMR experiments were performed at 223 K with a MAS frequency of 12 000 ± 5 Hz. The RFDR spectra were

acquired at a radio frequency of 188.64 MHz. TPPM was applied in all experiments to decouple protons in t_1, the RFDR mixing time, and during the acquisition time (*27*, *28*). The 90° proton pulse was set to 4.5 μs, ^{13}C B_1 fields of 50 kHz were used during the ramped CP sequence, and a 100 to 50% ramp was applied on the proton channel. Rotor-synchronized pulses with a length of 25 μs were used during the RFDR mixing time τ_m of 1.78 ms (*29*). In the t_2 dimension, 2K data points with a sweep with of 50 kHz were recorded. Zero-filling to 4K and an exponential line broadening of 25 Hz were applied prior to Fourier transformation.

The 2D HetCor spectra were obtained with PMLG decoupling during the t_1 period and a τ_m of 100 μs (*30*−*32*). In addition, the spectra were recorded with 1024 data points in t_2 and zero-filled to 2048 points. A Lorentz−Gauss window with the maximum at 0.1 of the acquisition time and a broadening of 100 Hz was applied prior to Fourier transformation. In the t_1 dimension, 64 points were recorded, which were zero-filled to 256 points, and a sine-square apodization was used.

^{1}H and ^{13}C shifts are relative to TMS, and are calibrated using the ^{1}H and ^{13}C signals from the phospholipids that are present in the isorhodopsin sample (*33*, *34*). The natural abundance ethylenic carbons of the phospholipid acyl chain that resonate with a σ_{lip}^C of 128.7 ppm are well-resolved in the 1D CP/MAS and 2D RFDR spectrum, while in the 2D ^{1}H−^{13}C HetCor spectrum of isorhodopsin, the methylenic phospholipid ^{1}H−^{13}C correlations with a σ_{lip}^C of 28.7 ppm are easily distinguished from the chromophore signals. This calibration method was recently validated in the study of rhodopsin (*16*). In the 2D HetCor spectrum, the correlations involving the acyllic and methylenic protons are also resolved. The lipid methylenic proton resonance is assigned to a σ_{lip}^H of 2.7 ppm, while a σ_{lip}^H of 5.3 ppm is attributed to the acyllic response. These two proton resonances were used to calculate a LG scaling factor of 0.59, which is well in line with the theoretical value of $1/\sqrt{3}$ [=0.577 (*31*)].

9-*cis*-Retinylidene model compounds were prepared and manipulated at temperatures below 0 °C in dim red light. Two equivalents of butylamine and 9-*cis*-retinal were dissolved in anhydrous diethyl ether (*35*). The solution was kept overnight at −20 °C over 4 Å molecular sieves and stirred. The *N*-(9-*cis*-retinylidene)butylimine SB was obtained after evaporation of the excess of butylamine and diethyl ether. The pSB was formed by the addition of 2 equiv of trifluoroacetic acid in water to a solution of the SB in diethyl ether at −20 °C. Evaporation of the solvent yielded the *N*-(9-*cis*-retinylidene)butyliminium trifluoroacetate as a dark-colored solid. The NMR data of the synthesized 9-*cis*-retinylidene compounds are summarized in Table 1.

To calculate $\Delta\sigma_{lig}^H$ and $\Delta\sigma_{lig}^C$ of the 9-*cis*-retinylidene chromophore in isorhodopsin, the ^{1}H and ^{13}C assignments of the prepared pSB model compound, *N*-(9-*cis*-retinylidene)-butyliminium trifluoroacetate, are used. With σ_{lig} representing the chemical shifts of the 9-*cis*-retinylidene chromophore in the active site and σ_{pSB} the shifts of a 9-*cis*-retinylidene pSB model compound in solution, the NMR ligation shifts are calculated from the relation $\Delta\sigma_{lig} = \sigma_{lig} - \sigma_{pSB}$ (*16*). Normalization of the $\Delta\sigma_{lig}^H$ and $\Delta\sigma_{lig}^C$ is performed to compensate for the large difference in the proton and carbon chemical shift scale. The scaling is accomplished according to the relations $\Delta\tilde{\sigma}_{lig}^H = \Delta\sigma_{lig}^H/15$ and $\Delta\tilde{\sigma}_{lig}^C = \Delta\sigma_{lig}^C/200$. The normalization facilitates comparison of the proton and carbon NMR ligation shifts. $\Delta\sigma_{lig}$ and $\Delta\tilde{\sigma}_{lig}$ are subsequently translated in the 9-*cis*-retinylidene chromophore, which is obtained using the structure of the 11-*cis*-retinylidene chromophore of the X-ray structure of rhodopsin (*36*, *37*). After a shift of the *cis* bond from 11-*cis* to 9-*cis*, in which all other spatial elements remained unaffected, the semiempirical calculation method MOPAC was used for the calculation of the minimal energy of a 9-*cis* model using the CS Chem3D Pro software package from CambridgeSoft. This model is used for the visualization of $\Delta\sigma_{lig}$ and $\Delta\tilde{\sigma}_{lig}$ in Figure 3.

Table 1: ^{1}H and ^{13}C Assignments of 9-*cis*-Retinal (ret), *N*-(9-*cis*-Retinylidene)-*n*-butylimine (SB), and *N*-(9-*cis*-Retinylidene)-*n*-butyliminium Trifluoroacetate (pSB)[a]

position	σ_{ret}^H (ppm)	σ_{ret}^C (ppm)	σ_{SB}^H (ppm)	σ_{SB}^C (ppm)	σ_{pSB}^H (ppm)	σ_{pSB}^C (ppm)
1	x	34.1	x	34.2	x	34.3
2	1.48	39.7	1.51	39.5	1.43	39.5
3	1.59	19.3	1.64	19.2	1.57	19.1
4	2.02	33.2	2.07	33.2	2.00	33.0
5	x	130.4	x	129.7	x	131.6
6	x	138.1	x	136.7	x	137.9
7	6.31	131.1	6.26	129.4	6.38	132.7
8	6.64	129.4	6.68	129.7	6.62	128.9
9	x	140.0	x	138.1	x	145.5
10	6.06	127.9	6.09	128.5	6.11	128.0
11	7.20	131.2	6.95	126.6	7.37	137.3
12	6.27	133.8	6.32	135.3	6.39	133.6
13	x	154.3	x	143.9	x	164.2
14	5.94	128.9	6.22	129.3	6.56	119.5
15	10.07	190.6	8.32	159.3	8.20	163.3
16/17	1.05	29.0	1.07	29.0	0.98	29.0
18	1.75	21.8	1.78	21.8	1.69	21.8
19	2.00	20.9	2.01	20.8	2.01	21.2
20	2.30	13.2	2.10	13.1	2.29	14.0
1′	x	x	3.51	61.8	3.60	52.4
2′	x	x	1.64	33.1	1.67	31.0
3′	x	x	1.38	20.5	1.32	19.4
4′	x	x	0.95	13.9	0.88	13.3

[a] The data were collected in $CDCl_3$ at room temperature using a Bruker 300 MHz DPX spectrometer. Shifts are reported in parts per million relative to TMS.

RESULTS

The 1D CP/MAS response of isorhodopsin reconstituted with the uniformly ^{13}C-labeled 9-*cis*-retinal is shown above the 2D homonuclear (^{13}C−^{13}C) and heteronuclear (^{1}H−^{13}C) correlation spectra in Figure 2. The broad signal at ∼175 ppm is derived from the natural abundance ^{13}C in the carbonyl moieties of the peptide bonds and the lipid esters. These have relatively weak spinning sidebands around 102 ppm. The two resonances (σ_{lig}^C = 169.6 ppm and σ_{lig}^C = 166.9 ppm) are from the two vinylic ^{13}C positions in the polyene that are shifted downfield due to high positive atomic charge densities (*16*). The other vinylic ^{13}C resonances resonate with shifts between 110 and 150 ppm. In this region, the natural abundance response of the unsaturated ^{13}C of the phospholipid acyl chain is also observed, with a σ_{lip}^C of 128.7 ppm. In the aliphatic region of the 1D spectrum, between 50 and 10 ppm, the methyl groups attached to the chromophore and the methylene carbon nuclei of the ionone moiety are clearly observable, superimposed on the natural abundance ^{13}C responses from the protein. For instance, the

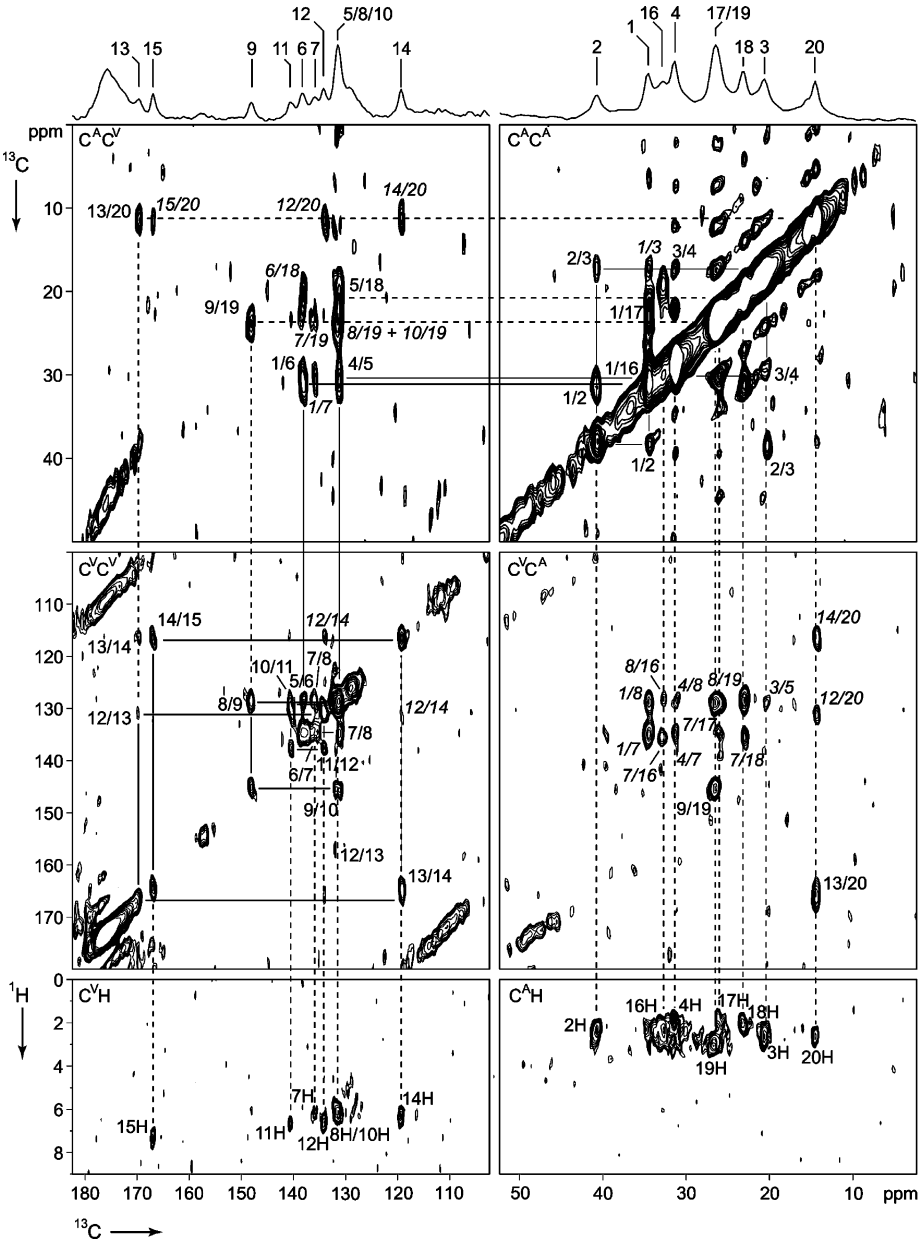

FIGURE 2: Contour regions of the 2D homonuclear ($^{13}C-^{13}C$) and 2D heteronuclear ($^1H-^{13}C$) dipolar correlation spectrum of isorhodopsin containing a uniformly ^{13}C-labeled chromophore, collected with a spinning frequency $\omega_r/2\pi$ of 12 000 ± 4 Hz. The regions shown in the top left (C^AC^V) and middle right panels (C^VC^A) display correlations between vinylic and aliphatic carbon nuclei. Correlations between vinylic carbons are shown in the middle left panel (C^VC^V), while couplings between aliphatic carbon nuclei are revealed in the top right panel (C^AC^A). In the bottom panels, the correlations between vinylic (C^VH) and aliphatic (C^AH) carbon nuclei and the attached protons are shown. Lines connecting the cross-peaks and diagonal peaks illustrate how they contribute to a correlation network. Nearest neighbor correlations are indicated with regular numbers, whereas italic numbers mark relayed transfer correlations.

shoulders on the signals with a $\sigma_{lig}{}^C$ of 20.5 ppm and a $\sigma_{lig}{}^C$ of 14.5 ppm are derived from side chains of aliphatic amino acids in isorhodopsin.

The incorporation of a uniformly ^{13}C-labeled chromophore enables the assignment of the NMR responses in a correlation spectroscopy experiment using broad band dipolar recoupling. In Figure 2, the relevant contour regions of the 2D homonuclear ($^{13}C-^{13}C$) and heteronuclear ($^1H-^{13}C$) correlation spectra of the 9-*cis* chromophore in isorhodopsin are shown. The signals on the diagonal in the RFDR spectrum correspond with the 1D NMR response of the ^{13}C nuclei shown at the top of Figure 2. The pairs of regular numbers indicate nearest neighbor correlation signals. The solid lines depict the correlation network for $^{13}C_1-^{13}C_{15}$ in the backbone of the 9-*cis*-retinylidene chromophore, while the dashed lines depict the correlations between the backbone and the directly attached methyl groups. In addition to nearest neighbor correlations, relayed cross-peaks are also detected, which are indicated with italic numbers. In particular, the saturated carbon nuclei of the chromophore show relatively strong relayed correlations with the nearby vinylic carbons. From the analysis of the 2D RFDR spectrum, the complete ^{13}C assignment of the chromophore of isorhodopsin is obtained (Table 2). The $\sigma_{lig}{}^C$ values for the nuclei of the polyene chain are generally in line with the assignments of Smith et al., within the experimental error of 1.2 ppm (Table 2) (*38*). The assignments of C7 and C19 (Table 2) are revised on the basis of the correlation data in Figure 2.

Table 2: Complete ^{13}C Assignment σ_{lig}^{C} of the 9-*cis*-Retinylidene Chromophore of Isorhodopsin Compared with σ_{pSB}^{C} for *N*-(9-*cis*-Retinylidene)-*n*-butyliminium Trifluoroacetate in Solution To Obtain the NMR Ligation Shift, $\Delta\sigma_{lig}^{C}$ [a]

position	σ_{lig}^{C} (ppm)	σ_{pSB}^{C} (ppm)	$\Delta\sigma_{lig}^{C}$ (ppm)	$\sigma_{lig,Ammonyx-LO}^{C}$ [b] (ppm)	$\Delta\sigma_{lig,rhodopsin}^{C}$ [c] (ppm)
1	34.4	34.3	0.1	x	−0.1
2	40.7	39.5	1.2	x	1.4
3	20.5	19.1	1.4	x	1.5
4	34.0	33.0	1.0	x	1.0
5	131.4	131.6	−0.2	130.5	−1.2
6	138.2	137.9	0.3	137.0	−0.2
7	135.8	132.7	3.1	128.2	0.5
8	131.1	128.9	2.2	131.1	1.9
9	148.0	145.5	2.5	147.5	1.2
10	131.3	128.0	3.3	130.8	1.5
11	140.5	137.3	3.2	139.3	2.7
12	134.1	133.6	0.5	133.9	3.5
13	169.6	164.2	5.4	169.2	2.5
14	119.1	119.5	−0.4	119.0	1.8
15	166.9	163.3	3.6	166.5	2.5
16	30.6	29.0	1.7	x	1.7
17	26.2	29.0	−2.8	x	−2.8
18	23.1	21.8	1.3	x	−0.4
19	26.6	21.2	5.4	19.8	1.8
20	14.5	14.0	0.5	13.6	−2.5

[a] The ^{13}C shifts of the polyene chain are also compared with the shifts collected in a stepwise approach using isorhodopsins that were solubilized in detergent (Ammonyx-LO) (*38*). [b] Data from ref *38*. [c] Data from ref *16*.

Table 3: Complete ^{1}H Assignment σ_{lig}^{H} of the 9-*cis*-Retinylidene Chromophore in Isorhodopsin[a]

position	σ_{lig}^{H} (ppm)	σ_{pSB}^{H} (ppm)	$\Delta\sigma_{lig}^{H}$ (ppm)	$\Delta\sigma_{lig,rhodopsin}^{H}$ [b] (ppm)
2	2.4	1.43	1.0	−0.5
3	2.6	1.57	1.0	0
4	2.3	2.00	0.3	−1.1
7	6.2	6.38	−0.2	−0.2
8	6.3	6.62	−0.3	−0.2
10	6.1	6.11	0	−0.6
11	6.6	7.37	−0.7	0.1
12	6.5	6.39	0.1	0.9
14	6.3	6.56	−0.3	0.3
15	7.3	8.20	−0.9	−1.1
16	2.2	0.98	1.2	−0.3
17	2.1	0.98	1.1	−0.5
18	2.2	1.69	0.5	−1.2
19	3.3	2.01	1.3	0.1
20	2.6	2.29	0.3	−0.9

[a] The data are compared with σ_{pSB}^{H} for *N*-(9-*cis*-retinylidene)-*n*-butyliminium trifluoroacetate in solution to obtain the NMR ligation shift, $\Delta\sigma_{lig}^{H}$. [b] Data from ref *16*.

Finally, the ^{13}C assignment can be exploited for an assignment of the proton resonances of the 9-*cis*-retinylidene chromophore. In the two bottom panels of Figure 2, the $^{1}H-^{13}C$ correlation signals of the 2D HetCor spectrum are shown. To detect predominantly the heteronuclear correlations between carbons and directly attached protons, a relatively short mixing time τ_m of 100 μs was used. On the basis of the ^{13}C assignment, a full assignment of the proton response was obtained (Table 3).

DISCUSSION

Due to recent improvements in technology, 2D MAS NMR dipolar correlation spectroscopy allows comprehensive chemical shift assignments of moderately sized multispin

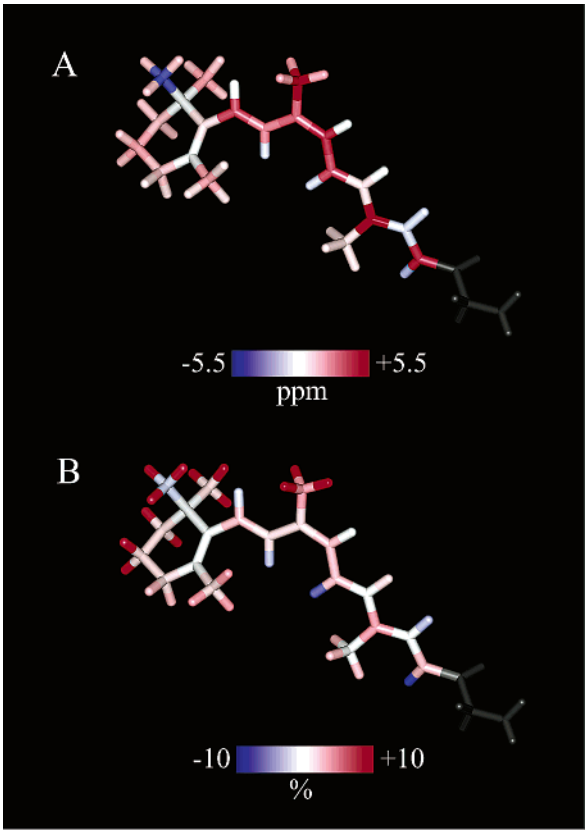

FIGURE 3: Visual presentation of (A) the $\Delta\sigma_{lig}^{C}$ and $\Delta\sigma_{lig}^{H}$ NMR ligation shifts shown in Tables 2 and 3 and (B) normalized $\Delta\tilde{\sigma}_{lig}^{C}$ and $\Delta\tilde{\sigma}_{lig}^{H}$. The blue and red colors reflect the upfield and downfield $\Delta\sigma_{lig}$, respectively (*16*).

^{13}C-labeled ligands bound to their membrane receptor target (*16*, *17*, *39*). The $\Delta\sigma_{lig}^{C}$ values provide detailed information about the electronic structure of the ligand in rhodopsin and confirm the excess of positive charge in the polyene originating from the pSB, yielding a polaronic conjugation defect close to the nitrogen of the pSB (*17*, *40*−*43*). It was verified that binding of the ligand to the protein results in a chiral selection by fixation of the ring puckering (*16*, *44*). This leads to equatorial and axial positions for the C16 and C17 methyl groups, respectively. In addition, the $\Delta\sigma_{lig}^{H}$ can be used to obtain information about nonbonding interactions between the ligand and the protein (*16*). For instance, considerable upfield $\Delta\sigma_{lig}^{H}$ values were observed for the protons of the methyl groups that are attached to the ionone ring of the chromophore of rhodopsin. These effects were attributed to ring current effects from nearby aromatic amino acids.

In Figure 3A, $\Delta\sigma_{lig}^{H}$ and $\Delta\sigma_{lig}^{C}$ for the 9-*cis*-retinylidene chromophore of isorhodopsin are visualized, while $\Delta\tilde{\sigma}_{lig}^{H}$ and $\Delta\tilde{\sigma}_{lig}^{C}$ are shown in Figure 3B (*16*). Like our previous study on rhodopsin, these images of the chromophore can be used to identify self-consistent patterns of NMR ligation shifts and to resolve details of the electronic and spatial structure of the ligand and of the ligand−protein interactions.

NMR Evidence for an Improper Fit of the Chromophore in Isorhodopsin. The C16 and C17 methyl groups of the 9-*cis*-retinylidene pSB model compound in solution resonate with a σ_{pSB}^{C} of 29.0 ppm (Table 1). In isorhodopsin, one of the resonances is detected with a σ_{lig}^{C} of 30.6 ppm, corresponding with a downfield $\Delta\sigma_{lig}^{C}$ of 1.7 ppm, while the other methyl resonates with a σ_{lig}^{C} of 26.2 ppm, resulting

Table 4: Chemical Shift Differences for the 9-*cis*-Retinylidene Chromophore in Isorhodopsin Relative to the Model Compounds 9-*cis*-β-Carotene ($\Delta\sigma_{Car}$), *N*-(9-*cis*-Retinylidene)butylimine ($\Delta\sigma_{SB}$), and *N*-(9-*cis*-Retinylidene)butyliminium Trifluoroacetate ($\Delta\sigma_{lig}$)

position	$\Delta\sigma_{Car}$[a] (ppm)	$\Delta\sigma_{SB}$ (ppm)	$\Delta\sigma_{lig}$ (ppm)
5	2.1	1.7	−0.2
6	0.2	1.5	0.3
7	7.5	6.4	3.1
8	1.1	1.4	2.2
9	13.4	9.9	2.5
10	2.0	2.8	3.3
11	16.6	13.9	3.2
12	−2.5	−1.2	0.5
13	33.2	25.7	5.4
14	−13.3	−10.2	−0.4
15	36.9	7.6	3.6
$\Delta\sigma^{total}$	97.2	59.5	23.5

[a] Data from ref *47*.

in an upfield $\Delta\sigma_{lig}^{C}$ of −2.8 ppm. The $\Delta\sigma_{lig}^{C}$ values for these methyl groups are attributed to intramolecular steric interactions with nearby carbons and protons of the β-ionone ring (*16*, *44*, *45*). Like rhodopsin, the binding site appears to inhibit the ring puckering motion of the chromophore in isorhodopsin (*16*, *44*, *46*).

Although a comparable ring conformation is present as in rhodopsin, the shift pattern for isorhodopsin reveals a global extended region of strong steric interactions and suggests an improper fit of the β-ionone ring in the binding site. The proton ligation shifts of C16 and C17 are comparable, exhibiting a relatively large downfield $\Delta\sigma_{lig}^{H}$ of 1.2 ppm and a $\Delta\sigma_{lig}^{H}$ of 1.1 ppm, respectively. A downfield $\Delta\sigma_{lig}^{H}$ of this magnitude indicates significant steric interactions between C16/C17 and the surrounding protein. The ligation shifts of other ring hydrogens support the interpretation in terms of significant steric interactions with the protein. The H2 and H3 protons shift downfield with a $\Delta\sigma_{lig}^{H}$ of 1.0 ppm, while the protons bound to C18 and C2−C4 are also shifted downfield. Finally, the carbon and the protons of C19 have downfield ligation shifts ($\Delta\sigma_{lig}^{C}$ = 5.4 ppm and $\Delta\sigma_{lig}^{H}$ = 1.3 ppm, respectively) that represent the largest $\Delta\sigma_{lig}^{C}$ and $\Delta\sigma_{lig}^{H}$ observed for the entire chromophore. Thus, an extended pattern of $\Delta\tilde{\sigma}_{lig}^{H}$ provides converging evidence for unspecific steric interactions and a misfit of the ring within the protein binding pocket.

Strain in the 9-cis-Retinylidene Chromophore of Isorhodopsin. A common property of retinal Schiff bases is an alternating pattern of positive charge at the odd-numbered carbons closest to the nitrogen in the form of a polaronic conjugation defect (*17*, *40*, *42*, *43*). By comparison of the data for the protein-bound ligand with the spectra collected from 9-*cis* model compounds of either the pSB, the unprotonated SB, or the β-carotene isomer, three levels of polarization effects on the polyene chain can be assessed (*17*). The chemical shift differences $\Delta\sigma_{lig}$, between the chromophore and the pSB model compound *N*-(9-*cis*-retinylidene)butyliminium trifluoroacetate, are listed in Table 4. The shifts suggest that isorhodopsin comprises a complex counterion environment similar to rhodopsin, where a hydrogen bond network involving a water molecule close to the positively charged pSB and a negatively charged carboxylate group of Glu113 are thought to interact with the polyene chain to stabilize positive charge density at C13 (*16*, *35*−*37*).

Both the formation of the SB and its protonation will affect the polarization of the polyene chain. The effect of protonation transpires from a comparison of the ^{13}C shifts of the chromophore with data for the unprotonated SB model compound *N*-(9-*cis*-retinylidene)butylimine (Table 4). Upon protonation, additional positive charge accumulates at the odd-numbered carbons close to the SB nitrogen. Using a conversion factor of 155 ppm/unit charge, we estimate that the excess charge on the olefinic carbons is ∼0.23 electronic equivalents. Finally, the effect of the formation of the SB on the polarization of the polyene chain is estimated from the ligand shifts of the chromophore relative to 9-*cis*-β-carotene (Table 4) (*47*). The introduction of an electronegative nitrogen leads to a polarization of ∼0.25 electronic equivalents of the ^{13}C close to the SB, largely accumulating at C13 and C15. This illustrates how SB formation can induce a polaronic conjugation defect. The ligation shifts in the C7−C10 region appear to be disconnected from the alternating charge effects at the Schiff base end. We consider these shifts anomalous and ascribe them primarily to chromophore distortions around the 9-*cis* bond. They provide evidence for strain in the isomerization region of the polyene and support the hypothesis that perturbation of the chromophore in the region of the *cis* bond induced by the protein environment assists the selective photoisomerization (*18*, *48*). The substantial downfield $\Delta\sigma_{lig}^{H}$ and $\Delta\sigma_{lig}^{C}$ of C19 corroborate this picture of global steric hindrance in the binding pocket. Such a strained 9-*cis* chromophore not only fully complies with our NMR data but also can explain the 5−10-fold slower regeneration rate and the 5 kcal lower binding enthalpy of the apoprotein for 9-*cis*-retinal than for 11-*cis*-retinal (*13*, *49*, *50*).

Isorhodopsin versus Rhodopsin. In rhodopsin, highly specific localized protein−ligand interactions were resolved by ^{1}H MAS NMR that are attributed to nonbonding interactions between the chromophore and side chains of protein residues. Most likely, the aromatic amino acid residues Phe208, Phe212, and Trp265 are in close contact with C16/C17 and C18 methyl groups, respectively (*16*). In addition, the $\Delta\tilde{\sigma}_{lig}^{C}$ of C16 and C17 showed that binding of the 11-*cis*-retinylidene chromophore results in a chiral selection by fixation of the ring puckering (*16*, *44*). Finally, while the upfield NMR ligation shifts of C20 were ascribed to a nonplanar conformation of the 12-s-*trans* bond originating from protein−ligand interactions, the NMR data gave no evidence for significant interactions between C19 and the protein (*16*). The data for the rhodopsin led us to conclude that the ionone moiety and 9-methyl group of the 11-*cis*-retinylidene chromophore fit tightly and precisely in the active site of the protein.

This strongly contrasts with isorhodopsin. Significant upfield $\Delta\sigma_{lig}^{H}$ values are observed only for H15 ($\Delta\sigma_{lig}^{H}$ = −0.9 ppm) and H11 ($\Delta\sigma_{lig}^{H}$ = −0.7 ppm). They can be ascribed to interactions with nearby aromatic amino acid side chains, which produce a ring current effect resulting in an upfield NMR ligation shift (*51*). In isorhodopsin, the $\Delta\sigma_{lig}^{H}$ values are predominantly downfield, for the protons attached to the ring moiety as well as for C19.

The shifts of C16 and C17 are very similar for rhodopsin and isorhodopsin, indicating that the upper part of the ring

adopts a similar fixed conformation in both pigments. Since both chromophores are covalently linked to Lys296 in a pSB and the ^{13}C shifts indicate a similar counterion environment, the pSB anchoring sites will also be at a very similar position in rhodopsin and isorhodopsin. Indeed, upon photoexcitation isorhodopsin will relax into the same bathorhodopsin intermediate as rhodopsin, with the lower photoisomerization quantum yield for the isorhodopsin species (*6*, *13*). We propose that upon binding both isomers induce a very similar conformation of the surrounding protein residues in the active site. With NMR, we however observe a very precise induced fit of the 11-*cis* chromophore in rhodopsin, while the general strain observed in isorhodopsin reveals a misalignment of the 9-*cis* chromophore in globally the same binding site, hence the term induced misfit.

Analysis of the origin of the positive charge delocalization within the 11-*cis*-retinylidene chromophore of rhodopsin and the 9-*cis*-retinylidene chromophore of isorhodopsin suggests that for both species the major effects of the charge delocalization can be ascribed to the formation and protonation of the SB and electrostatic interactions involving the C11−C13 region and a H-bonded counterion network, including water molecules and polar and/or negatively charged amino acid residues (*16*, *17*, *35*−*38*, *40*, *41*). Polarization by the electronegative SB nitrogen and the protonation of the SB give comparable effects for both chromophores. Hence, the shift of the *cis* bond has little effect on the polarization of the polyene chain. Verhoeven et al. observed a correlation between the polarization of the odd-numbered ^{13}C close to the SB ($\Delta\sigma_{odd}$) for the polyene chains of 11-*cis*-retinylidene species and the ν_{max} (*17*). The shift effects for C11, C13, and C15, which are attributed to positive charge delocalization in isorhodopsin, are well in line with the correlation between ν_{max} and $\Delta\sigma_{odd}$ previously established for the 11-*cis* form. In contrast, when the ^{13}C ligation shifts for C7 and C9 are included, the correlation breaks down. This supports our interpretation that the C7−C10 shifts are due to another mechanism: the intramolecular strain that is provoked by the induced misfit of the 9-*cis* chromophore.

CONCLUSIONS

High-field solid-state 2D homonuclear and heteronuclear MAS NMR dipolar correlation spectroscopy of isorhodopsin, reconstituted with uniformly 99% enriched ^{13}C-labeled 9-*cis*-retinal, allowed a complete ^{13}C and ^{1}H chemical shift assignment of the chromophore. $\Delta\sigma_{lig}$ and $\Delta\tilde{\sigma}_{lig}$ reflect the spatial and electronic structure of the chromophore in the active site of isorhodopsin relative to the 9-*cis*-retinylidene pSB model in solution and provide a global view of the mechanisms of ligand−protein interactions with atomic selectivity.

The NMR data indicate a similar counterion environment and ring position for rhodopsin and isorhodopsin. Distinct downfield ligation shifts are observed for the protons attached to the ionone moiety and C19, and are ascribed to significant steric interactions between the chromophore and the protein. The most straightforward explanation is that the ring, the 19-methyl group, and the Schiff base represent the major sites for chromophore recognition and interaction in opsin. While a similar protein binding pocket conformation is induced in rhodopsin and isorhodopsin, misalignment between the 9-*cis* configuration and the pocket provokes strain on the ring, on the 19-methyl group, and in the polyene chain 9-*cis* segment. The analysis of the $\Delta\sigma_{lig}^{C}$ pattern of the C7−C10 region is in line with a perturbation of the polyene chain. The nonspecific pattern of interactions for the isorhodopsin chromophore confirms that the fit of the 9-*cis*-retinylidene ligand into the opsin binding pocket is not optimal. This would explain biochemical observations such as a reduced binding enthalpy and slower binding kinetics for 9-*cis*-retinal.

ACKNOWLEDGMENT

We thank J. Hollander, C. Erkelens, and F. Lefeber for assistance with the MAS NMR experiments. Cambridge Isotope Laboratories is gratefully acknowledged for their kind gift of all ^{13}C-labeled starting materials that were used for the preparation of the uniformly ^{13}C-labeled retinal.

REFERENCES

1. Baldwin, J. M., Schertler, G. F. X., and Unger, V. M. (1997) An α-carbon template for the transmembrane helices in the rhodopsin family of G-protein-coupled receptors, *J. Mol. Biol. 272*, 144−164.
2. Baldwin, J. M. (1993) The probable arrangement of the helices in G protein-coupled receptors, *EMBO J. 12*, 1693−1703.
3. Pogozheva, I. D., Lomize, A. L., and Mosberg, H. I. (1997) The transmembrane 7-α-bundle of rhodopsin: Distance geometry calculations with hydrogen bonding constraints, *Biophys. J. 72*, 1963−1985.
4. Unger, V. M., Hargrave, P. A., Baldwin, J. M., and Schertler, G. F. X. (1997) Arrangement of rhodopsin transmembrane α-helices, *Nature 389*, 203−206.
5. Schoenlein, R. W., Petenau, L. A., Mathies, R. A., and Shank, C. V. (1991) The first step in vision: Femtosecond isomerization of rhodopsin, *Science 254*, 412−415.
6. Mathies, R. A., and Lugtenburg, J. (2000) The primary photoreaction of rhodopsin, in *Molecular Mechanisms in Visual Transduction* (Stavenga, D. G., DeGrip, W. J., and Pugh, E. N., Jr., Eds.) pp 55−90, Elsevier, Amsterdam.
7. Dartnall, H. J. A. (1972) in *Photochemistry of Vision* (Dartnall, H. J. A., Ed.) pp 122−145, Springer, Berlin.
8. Kandori, H., Matuoka, S., Nagai, H., Shichida, Y., and Yoshizawa, T. (1988) Dependency of apparent relative quantum yield of isorhodopsin to rhodopsin on the photon density of picosecond laser pulse, *Photochem. Photobiol. 48*, 93−97.
9. Kim, J. E., Tauber, M. J., and Mathies, R. A. (2001) Wavelength-dependent cis−trans isomerization in vision, *Biochemistry 40*, 13774−13778.
10. Liu, R. S. H. (1983) in *Frontiers in Biochemical and Biophysical Studies of Proteins and Membranes* (Liu, R. S. H., Ed.) pp 387−397, Elsevier, Amsterdam.
11. Makino, C. L., Kraft, T. W., Mathies, R. A., Miley, M. E., Van der Steen, R., and Baylor, D. A. (1990) Effects of modified chromophores on the spectral sensitivity of salamander, squirrel and macaque cones, *J. Physiol. 424*, 545−560.
12. VanHooser, J. P., Alemán, T. S., He, Y.-G., Cideciyan, A. V., Kuksa, V., Pittler, S. J., Stone, E. M., Jacobson, S. G., and Palczewski, K. (2000) Rapid restoration of visual pigment and function with oral retinoid in a mouse model of childhood blindness, *Proc. Natl. Acad. Sci. U.S.A. 97*, 8623−8628.
13. Liu, R. S. H., Crescitelli, F., Denny, M., Matsumoto, H., and Asato, A. E. (1986) Photosensitivity of 10-substituted visual pigment analogues: Detection of a specific secondary opsin-retinal interaction, *Biochemistry 25*, 7026−7030.
14. Hurley, J. B., Ebrey, T. G., Honig, B., and Ottolenghi, M. (1977) Temperature and wavelength effects on the photochemistry of rhodopsin, isorhodopsin, bacteriorhodopsin and their photoproducts, *Nature 270*, 540−542.
15. Smith, S. O., Courtin, J., de Groot, H. J. M., Gebhard, R., and Lugtenburg, J. (1991) ^{13}C magic-angle spinning NMR studies of bacteriorhodopsin, the primary photoproduct of rhodopsin, *Biochemistry 30*, 7409−7415.

16. Creemers, A. F. L., Kiihne, S., Bovee-Geurts, P. H. M., DeGrip, W. J., Lugtenburg, J., and de Groot, H. J. M. (2002) ^{1}H and ^{13}C MAS NMR evidence for pronounced ligand-protein interactions involving the ionone ring of the retinylidene chromophore in rhodopsin, *Proc. Natl. Acad. Sci. U.S.A. 99*, 9101−9106.
17. Verhoeven, M. A., Creemers, A. F. L., Bovee-Geurts, P. H. M., de Grip, W. J., Lugtenburg, J., and de Groot, H. J. M. (2001) Ultra-high-field MAS NMR assay of a multispin labeled ligand bound to its G-protein receptor target in the natural membrane environment: Electronic structure of the retinylidene chromophore in rhodopsin, *Biochemistry 40*, 3282−3288.
18. Carravetta, M., Zhao, X., Johannesen, O. G., Lai, W. C., Verhoeven, M. A., Bovee-Geurts, P. H. M., Verdegem, P. J. E., Kiihne, S., Luthman, H., de Groot, H. J. M., de Grip, W. J., Lugtenburg, J., and Levitt, M. H. (2004) Picometer structural resolution of a membrane protein ligand: Double-quantum solid-state NMR of bovine rhodopsin, *J. Am. Chem. Soc. 126* (in press).
19. Creemers, A. F. L., and Lugtenburg, J. (2002) The preparation of all-*trans* uniformly ^{13}C-labeled retinal via a modular total organic synthetic strategy, *J. Am. Chem. Soc. 124*, 6324−6334.
20. Feng, X., Verdegem, P. J. E., Lee, Y. K., Sandström, D., Edén, M., Bovee-Geurts, P., de Grip, W. J., Lugtenburg, J., de Groot, H. J. M., and Levitt, M. H. (1997) Direct determination of a molecular torsional angle in the membrane protein rhodopsin by solid-state NMR, *J. Am. Chem. Soc. 119*, 6853−6857.
21. Liu, R. S. H., and Asato, A. E. (1984) Photochemistry and synthesis of stereoisomers of vitamin A, *Tetrahedron 40*, 1931−1969.
22. DeGrip, W. J., Daemen, F. J. M., and Bonting, S. L. (1980) Isolation and purification of bovine rhodopsin, in *Methods in Enzymology*, Vol. 67, pp 301−320, Academic Press, New York.
23. De Lange, F., Bovee-Geurts, P. H., Van Oostrum, J., Portier, M. D., Verdegem, P. J., Lugtenburg, J., and De Grip, W. J. (1998) An additional methyl group at the 10-position of retinal dramatically slows down the kinetics of the rhodopsin photocascade, *Biochemistry 37*, 1411−1420.
24. De Grip, W. J. (1982) Purification of bovine rhodopsin over concanavalin A-sepharose, in *Methods in Enzymology*, Vol. 81, pp 197−207, Academic Press, New York.
25. Egorova-Zachernyuk, T. A., van Rossum, B., Boender, G.-J., Franken, E., Ashurst, J., Raap, J., Gast, P., Hoff, A. J., Oshkinat, H., and de Groot, H. J. M. (1997) NMR characterization of protein-pheophytin interactions in *Rhodobacter sphaeroides* R26 photosynthetic reaction centers, from multispin pheophytin enrichment and 2-D MAS NMR dipolar correlation spectroscopy, *Biochemistry 36*, 7513−7519.
26. Schulten, E. A. M., Matysik, J., Alia, Kiihne, S., Raap, J., Lugtenburg, J., Gast, P., Hoff, A. J., and de Groot, H. J. M. (2002) ^{13}C MAS NMR and photo-CIDNP reveal a pronounced asymmetry in the electronic ground state of the special pair of *Rhodobacter spheroides* reaction centers, *Biochemistry 41*, 8708−8717.
27. Pines, A., Gibby, M. G., and Waugh, J. S. (1973) Proton-enhanced NMR of dilute spins in solids, *J. Chem. Phys. 59*, 569−573.
28. Balaban, T. S., Holzwarth, A. R., Schaffner, K., Boender, G. J., and de Groot, H. J. M. (1995) CP-MAS ^{13}C NMR dipolar correlation spectroscopy of ^{13}C-enriched chlorosomes and isolated bacteriochlorophyll c aggregates of *Chlorobium tepidum*: The self-organization of pigments is the main structural feature of chlorosomes, *Biochemistry 34*, 15259−15266.
29. Boender, G. J., Raap, J., Prytulla, S., Oschkinat, H., and de Groot, H. J. M. (1995) MAS NMR structure refinement of uniformly ^{13}C enriched chlorophyll a/water aggregates with 2D dipolar correlation spectroscopy, *Chem. Phys. Lett. 237*, 502−508.
30. Van Rossum, B.-J., Boender, G. J., and de Groot, H. J. M. (1996) High magnetic field for enhanced proton resolution in high-speed CP/MAS heteronuclear $^{1}H-^{13}C$ dipolar-correlation spectroscopy, *J. Magn. Reson., Ser. A 120*, 274−277.
31. Van Rossum, B.-J., Förster, H., and de Groot, H. J. M. (1997) High-field and high-speed CP-MAS ^{13}C NMR heteronuclear dipolar-correlation spectroscopy of solids with frequency-switched Lee-Goldburg homonuclear decoupling, *J. Magn. Reson. 124*, 516−519.
32. Vinogradov, E., Madhu, P. K., and Vega, S. (1999) High-resolution proton solid-state NMR spectroscopy by phase-modulated Lee-Goldburg experiment, *Chem. Phys. Lett. 314*, 443−450.
33. Brown, M. F., Miljanich, G. P., and Dratz, E. A. (1977) Proton spin−lattice relaxation of retinal rod outer segment membranes and liposomes of extracted phospholipids, *Proc. Natl. Acad. Sci. U.S.A. 74*, 1978−1982.
34. .Zumbulyadis, N., and O'Brien, D. F. (1979) Proton and carbon-13 nuclear magnetic resonance studies of rhodopsin-phospholipid interactions, *Biochemistry 18*, 5427−5432.
35. Creemers, A. F. L., Klaassen, C. H. W., Bovee-Geurts, P. H. M., Kelle, R., Kragl, U., Raap, J., de Grip, W. J., Lugtenburg, J., and de Groot, H. J. M. (1999) ^{15}N solid-state NMR evidence for a complex Schiff base counterion in the visual G-protein coupled receptor rhodopsin, *Biochemistry 38*, 7195−7199.
36. Palczewski, K., Kumasaka, T., Hori, T., Behnke, C. A., Motoshima, H., Fox, B. A., Le Trong, I., Teller, D. C., Okada, T., Stenkamp, R. E., Yamamoto, M., and Miyano, M. (2000) Crystal structure of rhodopsin: A G-protein-coupled receptor, *Science 289*, 739−745.
37. Teller, D. C., Okada, T., Behnke, C. A., Palczewski, K., and Stenkamp, R. E. (2001) Advances in determination of a high-resolution three-dimensional structure of rhodopsin, a model of G-protein-coupled receptors (GPCRs), *Biochemistry 40*, 7761−7772.
38. Smith, S. O., Palings, I., Miley, M. E., Courtin, J., de Groot, H. J. M., Lugtenburg, J., and Mathies, R. A. (1990) Solid-state NMR studies of the mechanism of the opsin shift in the visual pigment rhodopsin, *Biochemistry 29*, 8155−8164.
39. Luca, S., White, J. F., Sohal, A. K., Filippov, D. V., Van Boom, J. H., Grishammer, R., and Baldus, M. (2003) The conformation of neurotensin bound to its G protein-coupled receptor, *Proc. Natl. Acad. Sci. U.S.A. 100*, 10706−10711.
40. Buda, F., de Groot, H. J. M., and Bifone, A. (1996) Charge localization and dynamics in rhodopsin, *Phys. Rev. Lett. 77*, 4474−4477.
41. Buda, F., Giannozzi, P., and Mauri, F. (2000) Density functional theory study of the structure and ^{13}C chemical shifts of retinylidene iminium salts, *J. Phys. Chem. B 104*, 9048−9053.
42. Bifone, A., de Groot, H. J. M., and Buda, F. (1997) Energy storage in the primary photoproduct of vision, *J. Phys. Chem. B 101*, 2954−2958.
43. La Penna, G., Buda, F., Bifone, A., and de Groot, H. J. M. (1998) The transistion state in the isomerization of rhodopsin, *Chem. Phys. Lett. 294*, 447−453.
44. Spooner, P. J. R., Sharples, J. M., Verhoeven, M. A., Lugtenburg, J., Claubitz, C., and Watts, A. (2002) Relative orientation of the β-ionone ring and polyenen chain for the chromophore of rhodopsin in native membranes, *Biochemistry 41*, 7549−7555.
45. Günther, H. (1995) in *NMR Spectroscopy*, 2nd ed., pp 501−504, John Wiley and Sons Ltd., Chichester, Great Britain.
46. Breitmaier, E., and Voelter, W. (1987) in *Carbon-13 NMR Spectroscopy*, 3rd ed., pp 115−116, VCH Verlagsgesellschaft, Weinheim, Germany.
47. Englert, G (1995) in *Carotenoids*, *Volume 1B: Spectroscopy*, pp 212, Birkhäuser Verlag, Basel, Switzerland.
48. Mathies, R., Freedman, T. B., and Stryer, L. (1977) Resonance Raman studies of the conformation of retinal in rhodopsin and isorhodopsin, *J. Mol. Biol. 109*, 367−372.
49. Cooper, A. (1979) Energy uptake in the first step of visual excitation, *Nature 282*, 531−533.
50. Cooper, A. (1979) Energetics of rhodopsin and isorhodopsin, *FEBS Lett. 100*, 382−384.
51. Giessner-Prettre, C., and Pullman, B. (1971) Intermolecular nuclear shielding due to the aromatic amino acids of proteins and to porphyrins, *J. Theor. Biol. 31*, 287−294.

BI048541E